



Implicit solvation based on generalized Born theory in different dielectric environments

Michael Feig, Wonpil Im, and Charles L. Brooks III

Citation: *The Journal of Chemical Physics* **120**, 903 (2004); doi: 10.1063/1.1631258

View online: <http://dx.doi.org/10.1063/1.1631258>

View Table of Contents: <http://scitation.aip.org/content/aip/journal/jcp/120/2?ver=pdfcov>

Published by the [AIP Publishing](#)

Articles you may be interested in

[Incorporating variable dielectric environments into the generalized Born model](#)

J. Chem. Phys. **122**, 094511 (2005); 10.1063/1.1857811

[Dielectric relaxation of electrolyte solutions using terahertz transmission spectroscopy](#)

J. Chem. Phys. **116**, 8469 (2002); 10.1063/1.1468888

[Dielectric response of concentrated NaCl aqueous solutions: Molecular dynamics simulations](#)

J. Chem. Phys. **115**, 1448 (2001); 10.1063/1.1381055

[Computer simulation of wavevector-dependent dielectric properties of polar and nondipolar liquids](#)

AIP Conf. Proc. **492**, 250 (1999); 10.1063/1.1301531

[Ewald artifacts in computer simulations of ionic solvation and ion-ion interaction: A continuum electrostatics study](#)

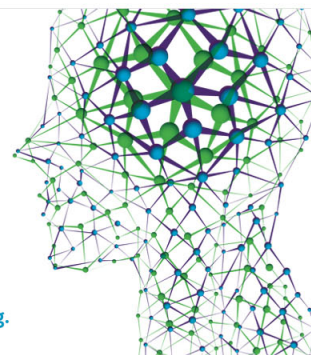
J. Chem. Phys. **110**, 1856 (1999); 10.1063/1.477873

How can you **REACH 100%**
of researchers at the Top 100
Physical Sciences Universities?
(TIMES HIGHER EDUCATION RANKINGS, 2014)

With *The Journal of Chemical Physics*.

AIP | The Journal of
Chemical Physics

THERE'S POWER IN NUMBERS. Reach the world with AIP Publishing.



Implicit solvation based on generalized Born theory in different dielectric environments

Michael Feig, Wonpil Im, and Charles L. Brooks, III^{a)}

Department of Molecular Biology, TPC6, The Scripps Research Institute, La Jolla, California 92037

(Received 31 July 2003; accepted 13 October 2003)

In this paper we are investigating the effect of the dielectric environment on atomic Born radii used in generalized Born (GB) methods. Motivated by the Kirkwood expression for the reaction field of a single off-center charge in a spherical cavity, we are proposing extended formalisms for the calculation of Born radii as a function of external and internal dielectric constants. We demonstrate that reaction field energies calculated from environmentally dependent Born radii lead to much improved agreement with Poisson–Boltzmann solutions for low dielectric external environments, such as biological membranes or organic solvent, compared to previous methods where the calculation of Born radii does not depend on the environment. We also examine how this new approach can be applied for the calculation of transfer free energies from vacuum to a given external dielectric for a system with an internal dielectric larger than one. This has not been possible with standard GB theory but is relevant when scoring minimized or average structures with implicit solvent. © 2004 American Institute of Physics. [DOI: 10.1063/1.1631258]

INTRODUCTION

It has long been appreciated that a realistic theoretical description of biologically relevant molecules has to account for the environment that is appropriate for a given system. When soluble molecules are considered, aqueous solvent is usually included either explicitly or implicitly.^{1,2} An accurate model of membrane-bound molecules, on the other hand, would require some representation of the anisotropic lipid environment, which is also possible either explicitly or implicitly.^{3–5} Furthermore, the generally dense packing of biological molecules in cellular compartments,⁶ where specific and nonspecific protein–protein and protein–nucleic acid interactions play an important role, warrants an appropriate description for molecules in such environments.

Specific, sterically dependent interactions between the environment and a molecule of interest usually require an explicit molecular representation. Examples of such cases are given by the highly immobilized and structured water molecules in the minor groove of DNA⁷ or cofactors or ligands that are essential components in many protein structures. Nonspecific solvent interactions lead to polarization effects according to the dielectric properties of the environment,² entropic penalties that arise when forming a cavity in a given environment,⁸ and van der Waals-type dispersion interactions with the molecules in the environment.⁹ In a good approximation these energetic contributions can be summarized with an implicit description that assumes a continuum model of the environment.¹⁰ The dominant electrostatic contribution due to polarization effects in such a continuum model is described rigorously through the Poisson equation¹¹

$$\nabla[\epsilon(\mathbf{r})\nabla\phi(\mathbf{r})] = -4\pi\rho(\mathbf{r}), \quad (1)$$

^{a)}Author to whom correspondence should be addressed. Electronic mail: brooks@scripps.edu

where the electrostatic potential $\phi(\mathbf{r})$ is related to a charge distribution $\rho(\mathbf{r})$ and space-dependent variation of the dielectric constant $\epsilon(\mathbf{r})$. In this model, different environments are characterized mainly by their dielectric response, with ϵ values ranging from 80 for water to 2–4 for the interior of lipid membranes. Solutions of $\phi(\mathbf{r})$ can then be used to calculate the solvent-induced reaction field energy for a system of interest in a given environment ($\epsilon = \epsilon_w$) with respect to a reference dielectric ($\epsilon = \epsilon_p$), e.g., vacuum ($\epsilon_p = 1$)

$$\Delta G_{\epsilon_p \rightarrow \epsilon_w}^{\text{elec}} = G_{\epsilon_w}^{\text{elec}} - G_{\epsilon_p}^{\text{elec}} \quad (2)$$

with the electrostatic energy calculated from an integral over all of space

$$G^{\text{elec}} = \frac{1}{2} \int_V \rho(\mathbf{r})\phi(\mathbf{r})dV. \quad (3)$$

An approximation to the reaction field energy can also be obtained with the generalized Born (GB) formalism in a pairwise sum over interacting charges^{12,13}

$$\Delta G_{\epsilon_p \rightarrow \epsilon_w}^{\text{elec}} = -\frac{1}{2} \left(\frac{1}{\epsilon_p} - \frac{1}{\epsilon_w} \right) \sum_{i,j} \frac{q_i q_j}{\sqrt{r_{ij}^2 + \alpha_i \alpha_j} \exp(-r_{ij}^2 / F \alpha_i \alpha_j)}, \quad (4)$$

where r_{ij} is the distance between atoms i and j , q_i and q_j are the respective (partial) charges, and α_i are the so-called generalized Born radii which may be interpreted roughly as the distance from each atom to the dielectric boundary. The factor F may range from 2 to 10 with 4 being the most commonly used value.¹³

Recent advances in GB methodology have resulted in excellent agreement between GB and Poisson–Boltzmann

(PB) energies^{14–18} with average relative errors of less than 1% for the GBMV method^{14–16} when calculating solvation energies of proteins in water. The application of implicit solvation descriptions has been increasingly successful in simulation studies,^{19,20} scoring of protein conformations,²¹ estimates of pK_a values,²² and evaluation of protein-ligand binding free energies.²³ However, since many biological processes occur in low-dielectric environments such as cell membranes, there is a strong incentive to extend continuum approaches based on GB to such environments as well. While efforts have been made in incorporating heterogeneous environments in GB-type formalisms,^{5,24} the extent to which existing GB formalisms are applicable to varying dielectric environments has not been addressed in detail.

Equation (4) is usually applied to a simple two-dielectric system where the set of charges occupies a molecular cavity with a dielectric constant ϵ_p surrounded by a uniform high-dielectric continuum environment with a dielectric constant ϵ_w . The prefactor $(1/\epsilon_p - 1/\epsilon_w)$ is motivated by the analysis of a single ion in a spherical cavity where it is rigorously correct for calculating the reaction field energy from a medium with ϵ_p to ϵ_w .^{18,25,26}

An internal dielectric of $\epsilon_p = 1$ is appropriate for dynamics simulations where dipole fluctuations occur explicitly as part of the model. A larger internal dielectric constant is more appropriate, though when the energies of minimized or averaged structures are evaluated. However, as illustrated elsewhere,²⁷ Equation (4) describes only the reaction field energy due to an external dielectric of ϵ_w with respect to a reference dielectric environment ϵ_p everywhere, inside and outside. GB theory cannot directly provide the transfer free energy from $\epsilon_p/1$ to ϵ_p/ϵ_w (internal/external dielectric constant).

The critical requirement for success of the generalized Born approximation lies in the efficient and accurate calculation of the atomic Born radii, α_i , in order to gain a computational advantage over costly solutions to the Poisson equation. According to the Coulomb field approximation, Born radii are commonly calculated from the following expression:²⁷

$$\frac{1}{\alpha_i} = A_4 \equiv \frac{1}{R_i} - \frac{1}{4\pi} \int_{\text{solute}, r > R_i} \frac{1}{r^4} dV, \quad (5)$$

where R_i are the atomic radii (e.g., van der Waals radius) used to define the solute cavity filling out the volume V , over which the integral is calculated. Recently, we have proposed a higher order correction term for an improved fit between Born radii calculated from GB and radii calculated directly from Poisson theory^{15,16}

$$A_7 = \left(\frac{1}{4R_i^4} - \frac{1}{4\pi} \int_{\text{solute}, r > R_i} \frac{1}{r^7} dV \right)^{1/4} \quad (6)$$

that is used in the following new parametrized expression for calculating the Born radii α_i :

$$\alpha_i = \frac{S}{C_0 A_4 + C_1 A_7} + D \quad (7)$$

with optimized values of $S=0.9114$, $C_0=0.2966$, $C_1=1.0369$, and $D=-0.0637$ from fitting solvation energies from Poisson theory for proteins with an interior dielectric constant of 1 and an exterior dielectric of 80 corresponding to water.

Born radii calculated from Eqs. (5) through (7) do not depend on the interior or exterior dielectric constants. The only place where the dielectric environment enters in generalized Born theory is through the prefactor $(1/\epsilon_p - 1/\epsilon_w)$ in Eq. (4). The treatment of the environment in Eq. (4) becomes problematic, however, if one attempts to calculate the transfer energy from vacuum to an environment with a dielectric constant ϵ_w for a system with an internal dielectric of ϵ_p as the transfer from $\epsilon_p/1$ to ϵ_p/ϵ_w (internal/external dielectric)

$$\begin{aligned} \Delta G_{\epsilon_p/1 \rightarrow \epsilon_p/\epsilon_w}^{\text{elec,GB}} &= \Delta G_{\epsilon_p/1 \rightarrow \epsilon_p/\epsilon_p}^{\text{elec,GB}} + \Delta G_{\epsilon_p/\epsilon_p \rightarrow \epsilon_p/\epsilon_w}^{\text{elec,GB}} \\ &= -\Delta G_{\epsilon_p/\epsilon_p \rightarrow \epsilon_p/1}^{\text{elec,GB}} + \Delta G_{\epsilon_p/\epsilon_p \rightarrow \epsilon_p/\epsilon_w}^{\text{elec,GB}} \\ &= -\frac{1}{2} \left(\frac{1}{\epsilon_p} - \frac{1}{1} \right) \Omega + \frac{1}{2} \left(\frac{1}{\epsilon_p} - \frac{1}{\epsilon_w} \right) \Omega \\ &= \frac{1}{2} \left(1 - \frac{1}{\epsilon_w} \right) \Omega. \end{aligned} \quad (8)$$

Here, Ω is used to denote the pairwise sum from Eq. (4). The analysis implies that the transfer energy from vacuum into a given environment would be independent of the internal dielectric constant. This paradox would be reconciled if the Born radii α_i varied as a function of the internal and external dielectric constants, which would result in values of Ω that now depend on ϵ_p and ϵ_w . For off-center charges and a nonspherical solute, the Born radii should in fact depend not just on the Coulomb field, which is environmentally independent, but also on the electric displacement due to the reaction field that arises as a result of the boundary between the different internal and external dielectric environments.^{28,29} Although the correction term in Eq. (6) was not derived rigorously as such, it can be viewed as representing the reaction field component for off-center charge locations in a cavity of arbitrary shape that is described incompletely by the Coulomb field approximation alone. While we will come back to this point in more detail below, it provides a route to introduce an explicit dependence on internal and external dielectric constants in Eq. (7) by changing the relative weight between A_4 and A_7 depending on ϵ in a way that would not be possible with Eq. (5) alone.

In this paper we will analyze the effect of different internal and external dielectric constants on the Born radii in more detail and propose new ways to extend the GB formalism to yield a more accurate treatment that allows application to systems with low external dielectric constants, such as in membrane environments, or the use of internal dielectric constants larger than 1 when scoring minimized or averaged conformations with GB.

METHODS

Calculation of transfer energies

Transfer energies were obtained from reaction field energies between different dielectric environments either by solving the Poisson equation (PB) or by applying a generalized Born (GB) formalism.

Transfer energies from PB solutions were used as reference values for GB calculations and obtained with the standard finite difference method implemented in the PBEQ module^{4,30,31} in CHARMM.³² A grid spacing of 0.25 Å was used in all cases. The molecular surface was used to define the dielectric boundary based on a spherical probe radius with a size of 1.4 Å. A margin of at least 4.5 Å from the extent of each structure to the edge of the grid was allowed in all cases to avoid boundary effects. Charges were distributed onto grid points using the trilinear interpolation method and successive over relaxation³³ was used to speed convergence, which was reached in all calculations. For the boundary potential a simple Coulomb term was calculated on every other grid point and interpolated for grid points in between.

Generalized Born results were obtained with the GBMV method^{15,16} in CHARMM, which implements Eqs. (4) and (7) and calculates the quantities A_4 and A_7 by carrying out the integration numerically rather than approximating the integral with a pairwise sum over atomic volumes, as in most other common GB implementations. For all GB calculations we used a regular angular integration grid with $N_\phi = 8$ (see Ref. 15) and a value of $F = 8$ in Eq. (4).

In both PB and GB calculations we used the charges from the CHARMM22 force field³⁴ and the standard van der Waals radii were used to define the molecular cavity and dielectric boundary. We did not consider salt effects in the present study. All of the calculations were performed using the ensemble computing facility of the MMTSB Tool Set.³⁵

Test sets

Three different test sets were employed in this study. Complete all-atom representations were generated for all of the structures without any minimization or refinement. Missing hydrogen atoms were added if necessary by using the HBUILD procedure in CHARMM.³² Explicit solvent molecules, ions or any co-ligands that may have been present in experimental structures were not included in the calculations. The test sets are available from the authors upon request.

Set 1 contains 22 native protein structures from the Protein Data Bank (PDB)³⁶ with less than 100 residues. These structures were used as the training set for some of the parameters in this study. The PDB codes for the structures in this set are given in the Appendix.

Set 2 contains a comprehensive set of 611 nonhomologous single-chain protein structures ranging from small protein fragments to very large structures with more than 800 residues and covering a wide variety of native folds. The PDB codes are also given in the Appendix.

Set 3 was used to test the calculation of transfer energies for different native and non-native conformations of the same protein, in this case the chicken villin headpiece (PDB code: 1VII). The test set consists of 120 near-native, mis-

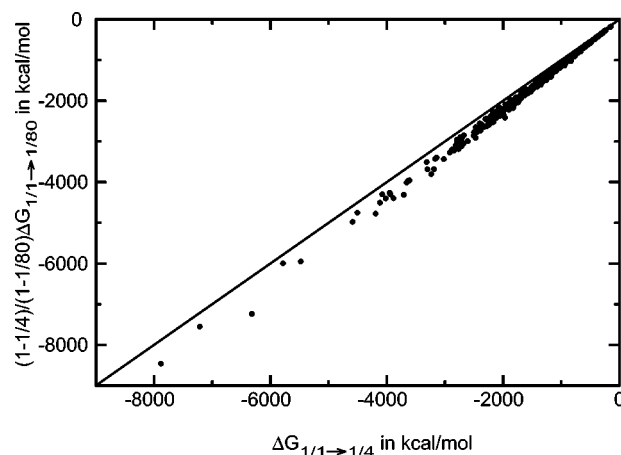


FIG. 1. Comparison of transfer free energies from 1/1 to 1/4 (internal/external dielectric) for 611 proteins in test set 2 calculated from PB directly and indirectly by multiplying $\Delta G_{1/1 \rightarrow 1/80}$ with $(1 - 1/4)/(1 - 1/80)$ according to Eq. (9).

folded, and unfolded conformations, generated through a lattice sampling protocol with low-resolution representations³⁷ followed by a subsequent reconstruction of all-atom models.³⁸

EXTENSION OF GENERALIZED BORN FORMALISM

Variation of dielectric environment

We begin by considering the effect of different dielectric constants ϵ_w for a homogenous continuum environment surrounding a molecular cavity with a set of partial charges q_i and an internal dielectric $\epsilon_p = 1$. Equation (4) implies that the reaction field energy for an environment with a dielectric constant of ϵ_w with respect to vacuum can be expressed as

$$\Delta G_{1/1 \rightarrow 1/\epsilon_w} = \left(1 - \frac{1}{\epsilon_w}\right) / \left(1 - \frac{1}{80}\right) \Delta G_{1/1 \rightarrow 1/80}. \quad (9)$$

One may calculate $\Delta G_{1/1 \rightarrow 1/80}$ from Poisson theory and compare $\Delta G_{1/1 \rightarrow 1/\epsilon_w}$ calculated according to Eq. (9) with reaction field energies obtained directly from Poisson theory for an external dielectric ϵ_w . Figure 1 shows the results for test set 2 (see methods section) when a value of 4 is chosen for ϵ_w . The values derived from $\Delta G_{1/1 \rightarrow 1/80}$ according to Eq. (9) generally correlate with the “correct” PB solutions, but a nonunity slope and noticeable scatter is found. This is quantified in more detail with the data given in Table I for different values of ϵ_w . We find that even if the nonunity slope is taken into account by scaling energies accordingly, relative errors of $> 2\%$ for low-dielectric environments are still quite large compared to an expected accuracy of $\sim 0.2\%$ for finite difference solutions to the Poisson equation with the 0.25 Å grid spacing used here.¹⁴

This observation confirms that the expression

$$\Delta G_{1/1 \rightarrow 1/\epsilon_w} = -\frac{1}{2} \left(1 - \frac{1}{\epsilon_w}\right) \cdot \Omega \quad (10)$$

TABLE I. Relative error in the calculation of transfer free energies $\Delta G_{1/1 \rightarrow 1/\epsilon_w}$ according to Eq. (9) from PB solutions for $\Delta G_{1/1 \rightarrow 1/80}$. The first value in each column was calculated with the factor $(1 - 1/\epsilon_w)/(1 - 1/80)$ as in Eq. (9). For the second value, the following scaling factors κ , obtained by linear regression of transfer energies for test set 2, were applied instead: $\kappa(\epsilon_w = 20)$: 0.943 36; $\kappa(\epsilon_w = 8)$: 0.842 21; $\kappa(\epsilon_w = 4)$: 0.693 80.

ϵ_w	Relative error in % $\Delta G_{1/1 \rightarrow 1/\epsilon_w}$ vs $\kappa \Delta G_{1/1 \rightarrow 1/80}$		
	Test set 1	Test set 2	Test set 3
20	0.46/0.53	1.10/0.45	0.21/0.12
8	1.29/1.39	2.99/1.21	0.58/0.30
4	2.51/2.50	5.67/2.29	1.11/0.55

with a constant quantity Ω is in fact not such a good approximation for polyionic systems occupying nonspherical cavities, and suggests that Ω should vary as a function of ϵ_w , as motivated in the introduction.

Instead of looking at reaction field energies for the entire system, one may also compare the atomic reaction field energy, $G_{\text{pol},i}$, for a unit charge at a given atomic site in the context of the solute cavity and the dielectric boundary without any additional charges present. The $G_{\text{pol},i}$ are related to atomic Born radii according to the Born equation²⁵

$$\alpha_i = -\frac{1}{2} \left(\frac{1}{\epsilon_p} - \frac{1}{\epsilon_w} \right) \frac{1}{G_{\text{pol},i}}. \quad (11)$$

Figure 2 shows a comparison of α_i that was calculated for one protein in test set 1 (1AJJ) according to Eq. (11) from $G_{\text{pol},i}$ values obtained by solving the Poisson equation between $\epsilon_w = 80$ and $\epsilon_w = 4$. It can be seen that the Born radii α_i vary as a function of ϵ_w rather than being constant as assumed in Eqs. (5) or (7). Furthermore, the application of Eq. (4) with the Born radii from PB theory for $\epsilon_w = 4$ results in a value of -547.4 kcal/mol for $\Delta G_{1/1 \rightarrow 1/4}$ in good agreement with a value of -558.1 kcal/mol from a direct PB solution for the entire molecule when $\epsilon_w = 4$. For comparison, a value of -599.4 kcal/mol is obtained if the Born radii for $\epsilon_w = 80$ are used in Eq. (4). This example indicates that Eq.

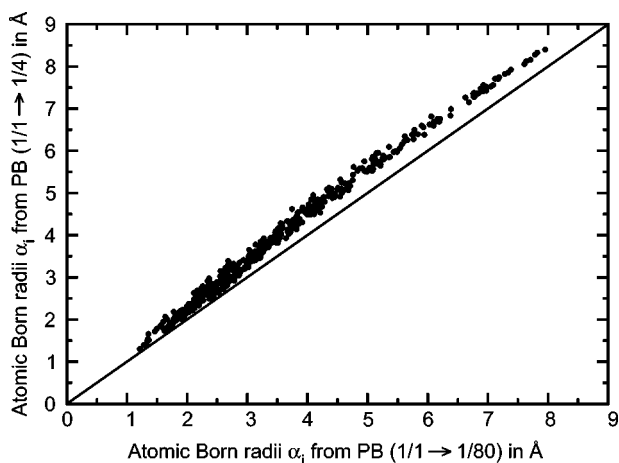


FIG. 2. Atomic Born radii α_i calculated based on Eq. (11) with $G_{\text{pol},i}$ from PB are compared between results obtained for external dielectric environments with $\epsilon_w = 4$ and 80.

(4) should remain valid for different environments as long as Born radii are used that depend on the environment in an appropriate manner. Consequently, the calculation of Born radii according to Eqs. (5) or (7) in the GB formalism should be extended to depend on ϵ_w with the Born radii calculated from PB for different values of ϵ_w as the reference.

In order to find an alternate expression for Eq. (7) that takes the effect of the environment into account in the calculation of Born radii, we will consider the case of a charge distribution in a spherical cavity with an internal dielectric ϵ_p and an external dielectric ϵ_w . In this case, the reaction field potential due to the presence of the dielectric boundary can be obtained as a closed form solution to the Poisson equation [Eq. (1)].²⁸ In a more convenient form of the original expression by Kirkwood, the reaction field potential for such a system at the location \mathbf{r} from the center of the spherical cavity with radius R can also be written as²⁹

$$\phi_{RF}(\mathbf{r}) = \sum_j^N -\frac{q_j}{2\epsilon_p} \sum_{l=0}^{\infty} \frac{(\ell+1)(\epsilon_w - \epsilon_p)}{(\ell+1)\epsilon_w + \ell\epsilon_p} \frac{r_j^\ell r^\ell}{R^{2\ell+1}} P_l(\cos \theta), \quad (12)$$

where the index j runs over all of the N charge sites at locations \mathbf{r}_j with charges q_j . P_l denotes the Legendre polynomial of order l , and θ is the angle between \mathbf{r}_j and \mathbf{r} . In the sum over l , the terms $l \neq 0$ are to be skipped either if $r_j = 0$ or $r = 0$.

In the case of a single, off-center charge q at a distance r from the center of a spherical cavity with radius R , Eq. (12) is reduced to

$$\phi_{RF}(\mathbf{r}) = -\frac{q}{2\epsilon_p} \sum_{l=0}^{\infty} \frac{(\ell+1)(\epsilon_w - \epsilon_p)}{(\ell+1)\epsilon_w + \ell\epsilon_p} \frac{r^{2l}}{R^{2l+1}} \quad (13)$$

and the reaction field energy when going from ϵ_p/ϵ_p to ϵ_p/ϵ_w is given as

$$\begin{aligned} \Delta G_{\epsilon_p/\epsilon_p \rightarrow \epsilon_p/\epsilon_w}^{\text{elec}} &= q \phi_{RF}(\mathbf{r}) \\ &= -\frac{q^2}{2} \left(\frac{1}{\epsilon_p} - \frac{1}{\epsilon_w} \right) \left(\frac{1}{R} + \frac{2\epsilon_w}{2\epsilon_w + \epsilon_p} \frac{r^2}{R^3} \right. \\ &\quad \left. + \frac{3\epsilon_w}{3\epsilon_w + 2\epsilon_p} \frac{r^4}{R^5} + \dots \right). \quad (14) \end{aligned}$$

While the familiar result of the Born equation for a single ion at the center of a spherical cavity²⁵ is recovered for $r=0$, additional terms, that depend on both ϵ_w and ϵ_p , are introduced when the charge is located off center ($r > 0$).

It is instructive to compare Eq. (14) with the calculation of reaction field energies from Eq. (11) when Born radii from GB theory according to Eq. (7) are used. Figure 3 shows results for transfer from vacuum to $\epsilon_w = 80$ for the case of a unit charge at distance r from the center of a spherical cavity. We find that the overall agreement between the exact result according to Eq. (14) and the result from GB is reasonable. However, it is most interesting to examine how the individual components C_0A_4 and C_1A_7 in Eq. (7) vary as a function of r . As can be seen in Fig. 3, C_0A_4 provides a nearly constant contribution with increasing distance from the center while C_1A_7 based on the new correction term

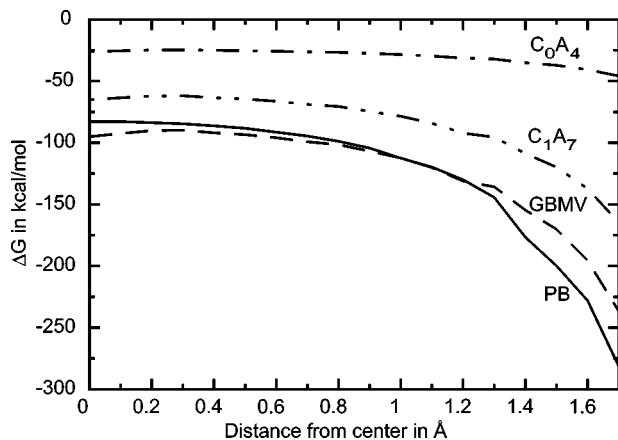


FIG. 3. Transfer free energies for $\epsilon_p = 1$ and $\epsilon_w = 80$ for a single unit charge in a spherical cavity of radius 2 Å as a function of distance from the center. Results from PB theory [which are very similar to the exact solution according to Eq. (14)] are compared to GBMV results as well as the individual contributions from the components C_0A_4 and C_1A_7 according to Eq. (7).

depends much more strongly on the distance r . When compared to Eq. (14), C_0A_4 may be related to the contribution from the spherically centered Born term ($l=0$), while C_1A_7 can be viewed as summarizing the higher order off-center contributions ($l>0$). This analogy then provides the motivation for introducing ϵ_p and ϵ_w in the calculation of Born radii by using a prefactor of

$$\frac{(n+1)\epsilon_w}{(n+1)\epsilon_w + n\epsilon_p}$$

for the C_1A_7 term in Eq. (7) as in Eq. (14) for the higher-order terms. We found excellent results with $n=2$, resulting in the following new expression for calculating Born radii:

$$\alpha_i = \frac{1}{C_0A_4 + C_1\left(\frac{3\epsilon_w}{3\epsilon_w + 2\epsilon_p}\right)A_7} + D + \frac{E}{\epsilon_w + 1} \quad (15)$$

with optimized values of $C_0=0.3255$, $C_1=1.085$, $D=-0.14$, and $E=-0.15$ based on the training set, test set 1.

The introduction of the term $E/(\epsilon_w + 1)$ improves results slightly over a constant shift D that is independent of ϵ_w . In general, a nonzero shift of Born radii is introduced mainly in order to match results from PB with a given grid resolution. The best shift for optimal agreement between GB and PB results is in fact reduced towards zero when matching PB results obtained at very high grid resolutions (e.g., 0.1 Å). In this context, the term $E/(\epsilon_w + 1)$ may be seen as a reflection of different levels of PB convergence depending on ϵ_w at a given grid resolution due to the extent of electrostatic effects as a function of dielectric screening. This point is illustrated conveniently with the simple case of a unit charge at the center of a spherical cavity where the Born radius is exactly equal to the radius of the spherical cavity. Figure 4 shows how Born radii calculated from PB according to Eq. (11) deviate from the exact result as a function of the external dielectric at different grid resolutions.

When Eq. (15) is applied for the calculation of GB radii, we find that the agreement with PB radii is significantly im-

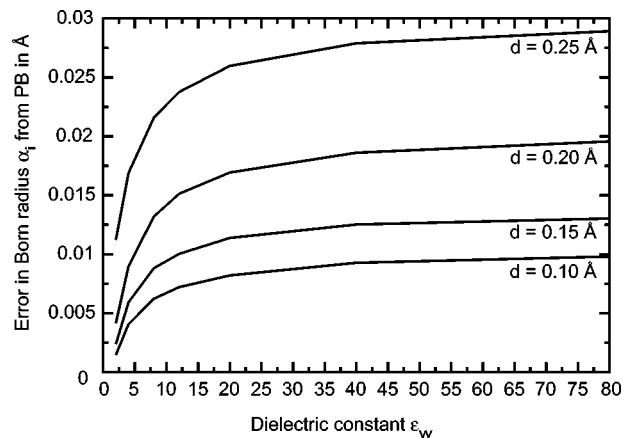


FIG. 4. Error in the calculation of Born radii calculated according to Eq. (11) from PB for the case of a single ion in a sphere of radius 2 Å as a function of the external dielectric ϵ_w and PB grid spacing d .

proved over Eq. (7) as shown in Fig. 5 for the test system 1AJJ and values of $\epsilon_w=4$ and $\epsilon_p=1$. Environmentally dependent Born radii according to Eq. (15) also translate into more accurate reaction field energies for entire molecules when Eq. (4) is applied. Table II compares reaction field energies when going from ϵ_p/ϵ_p to ϵ_p/ϵ_w (internal/external dielectric) for different combinations of ϵ_w and ϵ_p between PB and GB for the three protein-structure test sets (see Methods) used in this study. We find that relative errors vary only slightly across a wide range of dielectric environments and generally remain near 1% when Born radii are calculated from Eq. (15). For comparison, Table II also shows the relative errors that are obtained according to Eq. (4) if Born radii are not adjusted according to Eq. (15). The data show a clear improvement of the new formalism proposed here that is most apparent for small values of ϵ_w and large values of ϵ_p .

Variation of internal dielectric

We will now discuss how the GB formalism may be used to calculate transfer free energies for a system with an arbitrary internal dielectric ϵ_p from vacuum to a given exter-

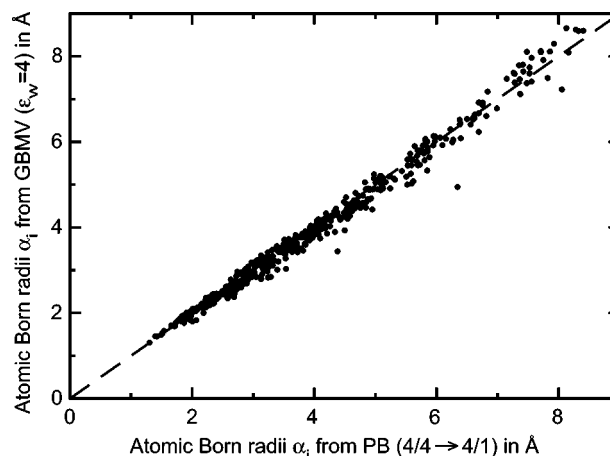


FIG. 5. Atomic Born radii, α_i , calculated with GBMV based on Eq. (15) for $\epsilon_w=4$ are compared against Born radii based on Eq. (11) with $G_{\text{pol},i}$ from PB for $\epsilon_w=4$. The correlation coefficient is 0.994.

TABLE II. Relative error in the calculation of transfer free energies $\Delta G_{\varepsilon_p/\varepsilon_p \rightarrow \varepsilon_p/\varepsilon_w}$ between GB with Born radii obtained according to Eq. (15) and PB solutions for different combinations of ε_p and ε_w . Numbers in parentheses indicate relative errors from using the original GB formalism based on Eq. (4) where the dependence on ε_p and ε_w is only taken into account through the prefactor $(1/\varepsilon_p - 1/\varepsilon_w)$, while Born radii for $\varepsilon_p = 1$ and $\varepsilon_w = 80$ are used.

		Relative error in % $\Delta G_{\varepsilon_p/\varepsilon_p \rightarrow \varepsilon_p/\varepsilon_w}$ GB vs PB		
ε_p	ε_w	Test set 1	Test set 2	Test set 3
1	80	1.10	0.94	0.43
1	20	1.06 (1.27)	0.90 (1.07)	0.41 (0.54)
1	8	1.01 (1.84)	1.05 (2.65)	0.45 (0.84)
1	4	1.07 (2.76)	1.37 (5.26)	0.62 (1.34)
2	80	1.07 (1.16)	0.92 (0.85)	0.41 (0.46)
4	80	1.04 (1.27)	0.93 (1.07)	0.39 (0.54)
8	80	0.98 (1.65)	1.01 (2.10)	0.42 (0.74)
4	20	1.01 (2.38)	1.27 (4.25)	0.57 (1.15)

nal dielectric ε_w , i.e., $\Delta G_{\varepsilon_p/1 \rightarrow \varepsilon_p/\varepsilon_w}$. As mentioned previously, this is not straightforward since the internal dielectric constant does not appear explicitly in GB theory. However, one may calculate the total transfer energy $\Delta G_{\varepsilon_p/1 \rightarrow \varepsilon_p/\varepsilon_w}$ as follows:

$$\Delta G_{\varepsilon_p/1 \rightarrow \varepsilon_p/\varepsilon_w} = \Delta G_{\varepsilon_p/1 \rightarrow \varepsilon_p/\varepsilon_p} + \Delta G_{\varepsilon_p/\varepsilon_p \rightarrow \varepsilon_p/\varepsilon_w}. \quad (16)$$

While the second term $\Delta G_{\varepsilon_p/\varepsilon_p \rightarrow \varepsilon_p/\varepsilon_w}$ may be calculated as outlined above, we will focus now on how to obtain the first term $\Delta G_{\varepsilon_p/1 \rightarrow \varepsilon_p/\varepsilon_p}$ from GB. In principle, $\Delta G_{\varepsilon_p/1 \rightarrow \varepsilon_p/\varepsilon_p} = -\Delta G_{\varepsilon_p/\varepsilon_p \rightarrow \varepsilon_p/1}$ should follow the calculation of $\Delta G_{\varepsilon_p/\varepsilon_p \rightarrow \varepsilon_p/\varepsilon_w}$, where $\varepsilon_w = 1$ and $\varepsilon_p > \varepsilon_w$. We found, however, that simply using Eq. (15) with appropriate values for ε does not produce satisfactory results. Instead, a slightly different form of Eq. (15) appears to be better suited for calculating Born radii in the case of $\Delta G_{\varepsilon_p/\varepsilon_p \rightarrow \varepsilon_p/1}$, which is given in the following:

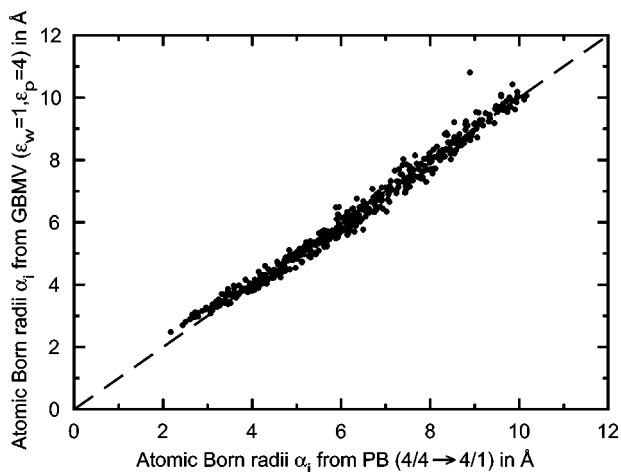


FIG. 6. Atomic Born radii α_i calculated with GBMV based on Eq. (17) for $\varepsilon_p = 4$ are compared against Born radii based on Eq. (11) with $G_{\text{pol},i}$ from PB for $\varepsilon_p = 4$ and $\varepsilon_w = 1$. The correlation coefficient is 0.992. The shift in radii from GB vs PB was introduced to improve the agreement of molecular transfer energies.

TABLE III. Relative error in the calculation of transfer free energies $\Delta G_{\varepsilon_p/\varepsilon_p \rightarrow \varepsilon_p/1}$ between GB with Born radii obtained according to Eq. (17) ($D = -0.55$) and PB solutions for different values of ε_p .

ε_p	Relative error in % $\Delta G_{\varepsilon_p/\varepsilon_p \rightarrow \varepsilon_p/1}$ GB vs PB		
	Test set 1	Test set 2	Test set 3
2	1.93	3.53	2.25
4	3.27	5.32	3.32
8	5.63	7.93	4.91

$$\alpha_i = \frac{1}{C_0 A_4 + C_1 \left(\frac{1}{1 + \varepsilon_p} - 1 \right) A_7} + D + E \varepsilon_p$$

$$= \frac{1}{C_0 A_4 + C_1 \left(\frac{-\varepsilon_p}{1 + \varepsilon_p} \right) A_7} + D + E \varepsilon_p, \quad (17)$$

where $\varepsilon_w = 1$ is assumed and the parameters are $C_0 = 1.2390$, $C_1 = 0.4592$, $D = -0.25$, and $E = 0.20$ as optimized from comparing Born radii between PB and GB. When optimized for the calculation of molecular transfer energies in the training set, $D = -0.55$ gives better results. Following Eq. (17), atomic Born radii can be calculated with the GB formalism that agrees well with atomic radii from PB for the transfer from $\varepsilon_p/\varepsilon_p$ to $\varepsilon_p/1$ as shown in Fig. 6. Surprisingly, though, when Born radii are calculated according to Eq. (17) and used in Eq. (4) with $\varepsilon_w = 1$ to obtain molecular transfer energies $\Delta G_{\varepsilon_p/\varepsilon_p \rightarrow \varepsilon_p/1}$ for the three test sets, the agreement between GB and PB is quite poor (see Table III) compared to the level of accuracy that is usually achieved with the GBMV method used here.¹⁴ While this may be due in part to less accurate Born radii, we find that even if we use “perfect” Born radii from PB in Eq. (4) the agreement with direct PB solutions is of similar (poor) quality. For test set 1 the relative error is $\sim 4\%$ (see Fig. 7). This observation leads us to believe that Eq. (4), which reproduces transfer energies from $\varepsilon_p/\varepsilon_p$ to $\varepsilon_p/\varepsilon_w$ very well, as long as accurate Born radii are used as input,³⁹ does not hold up to the same degree

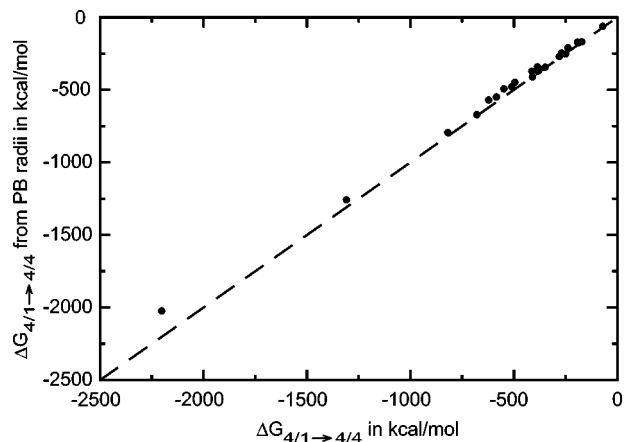


FIG. 7. Transfer free energies $\Delta G_{4/1 \rightarrow 4/4}$ obtained directly from PB solutions compared with calculations according to Eq. (4) with atomic Born radii α_i from PB for structures in test set 1.

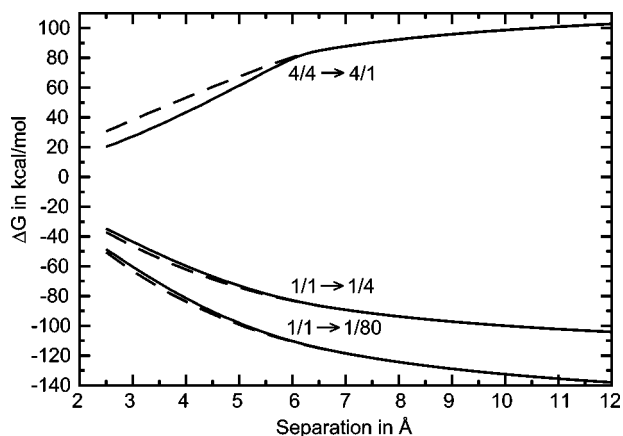


FIG. 8. Reaction field energies for two opposite unit charges in spheres of radius 2 Å as a function of separation for transfer from 1/1 to 1/4, 1/1 to 1/80, and 4/4 to 4/1 (internal/external dielectric). PB solutions are shown as solid lines. Solutions according to Eq. (4) with Born radii α_i calculated from PB are shown as dashed lines.

of accuracy when $\epsilon_w < \epsilon_p$ and in particular $\epsilon_w = 1$. The point is illustrated further by analyzing a simple model system consisting of two point charges with opposite unit charges embedded in spheres of radius 2 Å. Figure 8 shows how the transfer free energies $\Delta G_{4/4 \rightarrow 4/1}$, $\Delta G_{4/4 \rightarrow 4/80}$, and $\Delta G_{1/1 \rightarrow 1/80}$, obtained from PB and calculated via Eq. (4) with appropriate Born radii from PB, vary as a function of distance. Significant deviations are apparent below 6 Å in the case of $\Delta G_{4/4 \rightarrow 4/1}$ between values calculated from Eq. (4) and direct PB solutions.

A correction of this problem would require modification of Eq. (4). We have attempted to extend the pairwise expression based on earlier suggestions²² as well as new ideas, but did not find a satisfactory expression that improves the calculation of transfer energies of polyionic molecular systems beyond the training set that was used. There are some indications, however, that a three-body expression may be more successful (data not shown), but such expressions would carry significantly higher computational costs and render GB methods computationally unattractive compared to PB. Clearly, more work is required here to better understand and address this issue.

While the calculation of $\Delta G_{\epsilon_p/\epsilon_p \rightarrow \epsilon_p/1}$ is unsatisfactory by itself, it still leads to acceptable errors if combined with $\Delta G_{\epsilon_p/\epsilon_p \rightarrow \epsilon_p/\epsilon_w}$ for calculating transfer energies from $\epsilon_p/1$ to ϵ_p/ϵ_w according to Eq. (16). The accuracy of total transfer energies from vacuum to $\epsilon_w = 80$ obtained with GB theory for different internal dielectrics of $\epsilon_p = 2, 4$, and 8 are given in Table IV. At least up to $\epsilon_p = 4$ relative errors in calculating $\Delta G_{\epsilon_p/1 \rightarrow \epsilon_p/\epsilon_w}$ are 2%–3%. This may be sufficient for some applications such as the scoring of minimized or averaged protein structures, where an internal dielectric of 2 or 4 is more appropriate.

DISCUSSION AND CONCLUSIONS

Both GB and PB methods follow the same underlying physical model of a set of charges within a molecular cavity that is surrounded by a continuous dielectric media. While PB theory based on Eq. (1) describes such a system rigorously,

TABLE IV. Relative error in the calculation of transfer free energies $\Delta G_{\epsilon_p/1 \rightarrow \epsilon_p/80}$ between GB results obtained from $-\Delta G_{\epsilon_p/\epsilon_p \rightarrow \epsilon_p/1} + \Delta G_{\epsilon_p/\epsilon_p \rightarrow \epsilon_p/80}$ with Born radii obtained according to Eqs. (15) and (17) ($D = -0.55$) and direct PB solutions.

ϵ_p	Relative error in % $\Delta G_{\epsilon_p/1 \rightarrow \epsilon_p/80}$ GB vs PB		
	Test set 1	Test set 2	Test set 3
2	0.99	1.62	0.98
4	2.08	3.58	2.04
8	4.49	7.67	3.68

ously, GB formalisms aim at providing approximate transfer or solvation energies from vacuum to the given environment at much reduced cost. Consequently, solutions from PB theory constitute the natural reference point for transfer energies calculated through GB methods, although, ultimately, both PB and GB theory have to be compared against experimental data as well as explicit solvent simulations in order to judge the success of a continuum approach in describing environmental effects for molecular systems.

In the present study we have analyzed GB theory in comparison with transfer energies obtained from PB as a function of high and low external and internal dielectric constants. We found that an accurate account of the environment requires that the atomic Born radii are adjusted according to the dielectric environment. Motivated by the analytical expression for the reaction field of a set of charges in a spherical cavity that was derived originally by Kirkwood,²⁸ we have extended the calculation of Born radii in the GBMV method to reflect a dependence on the internal and external dielectric constants ϵ_p and ϵ_w for off-center charge distributions in a given molecular cavity. When Born radii are calculated according to this new GB formalism and applied in Eq. (4) to obtain molecular transfer free energies, we are able to reproduce PB transfer free energies between ϵ_p/ϵ_p and ϵ_p/ϵ_w for different dielectric environments much more accurately than with Born radii that are environmentally independent. This new approach extends GB-type methods to implicit modeling of low-dielectric environments. It is particularly attractive for the modeling of membrane environments, but it also enables applications involving low-dielectric solvent such as cyclohexane, ethanol, or octanol, to the extent that an implicit treatment of these solvents is adequate. We should point out, though, that for any of these types of environments, the radius of the solvent probe molecule, which is used to define the molecule surface, would have to be adjusted accordingly. All of the transfer free energies calculated in this study were based on a probe radius of 1.4 Å, which is meant to approximate the size of a water molecule. In other types of environments this radius would have to be adjusted to reflect the size of the solvent molecules that are involved. Since we have been comparing transfer energies in this study only between GB and PB rather with experimental data or explicit solvent simulations, we contend that our results are meaningful irrespective of the chosen probe radius.

Another caveat for the practical application of the new method described here concerns the choice of atomic radii

that are used to define the molecular surface. Van der Waals radii from a given force field may be used as a default, but since they are usually optimized for solute interactions as well as interactions with a certain explicit water model, they are not necessarily applicable to an implicit treatment of the environment. In fact, adjustment of atomic radii for the purpose of defining the dielectric boundary has been found to improve the calculation of solvation free energies in water,^{8,20,31} and similar adjustments are likely needed for other types of environments as well, in order to match experimental data and/or explicit simulations of the environment.

We have also examined the calculation of transfer energies $\Delta G_{\epsilon_p/\epsilon_p \rightarrow \epsilon_p/1}$ with a GB formalism. In this case, Born radii can be calculated fairly well with a slightly modified and reparametrized version of Eq. (15). However, we find that the pairwise sum approximation in Eq. (4) is not as successful in the case of $\epsilon_w < \epsilon_p$ as when calculating $\Delta G_{\epsilon_p/\epsilon_p \rightarrow \epsilon_p/\epsilon_w}$ where $\epsilon_w > \epsilon_p$. Consequently, molecular transfer free energies calculated according to Eq. (4) carry significantly larger errors compared to PB results. While further work will be concentrated on modifying Eq. (4) in order to address this problem, one may combine the approximate estimates of $\Delta G_{\epsilon_p/\epsilon_p \rightarrow \epsilon_p/1}$ with more accurate values of $\Delta G_{\epsilon_p/\epsilon_p \rightarrow \epsilon_p/\epsilon_w}$ in order to obtain transfer energies $\Delta G_{\epsilon_p/1 \rightarrow \epsilon_p/\epsilon_w}$ with an error of 2%–3%. While the calculation of transfer energies from vacuum to a medium with an external dielectric ϵ_w for a set of charges embedded in a low dielectric $\epsilon_p > 1$ is not possible with previous GB methods, such solvation energies are most appropriate for the scoring of minimized or averaged conformations. Potential applications lie in structure prediction or protein-ligand docking, where a reduced accuracy may be acceptable. It should be pointed out, however, that it would be possible to work around the limitations of the GB formalism in reproducing $\Delta G_{\epsilon_p/1 \rightarrow \epsilon_p/\epsilon_w}$ by choosing a reference state of ϵ_p/ϵ_p rather than vacuum while calculating the Coulomb energy with a dielectric constant of ϵ_p to be consistent.

ACKNOWLEDGMENT

Financial support from the NIH supported resource Multiscale Modeling Tools in Structural Biology (<http://mmts.scripps.edu>) (Grant No. RR12255) is acknowledged.

APPENDIX: PDB ENTRY CODES AND CHAIN ID FOR PROTEIN TEST SETS

PDB codes, test set 1

1AJJ, 1BBL, 1BOR, 1BPI, 1CBN, 1FCA, 1FRD, 1FXD, 1HPT, 1MBG, 1NEQ, 1PTQ, 1R69, 1SH1, 1SVR, 1TSG, 1UXC, 1VII, 1VJW, 2ERL, 2PDE, 451C.

PDB codes, test set 2

1A23, 1A2S, 1A5R, 1A63, 1A66_A, 1A6B_B, 1A6S, 1A7M, 1A91, 1A93_A, 1A93_B, 1A9V, 1AA3, 1AB3, 1AB7, 1ABT_A, 1ABV, 1ABZ, 1AC0, 1ACA, 1ACI, 1ADN, 1ADR, 1AF8, 1AFH, 1AFO_A, 1AGG, 1AH2, 1AH9, 1AHL, 1AIW, 1AJ3, 1AJE, 1AJW, 1AJY_A, 1AK6,

1AKP, 1AML, 1AO8, 1AOY, 1AP0, 1AP7, 1AP8, 1APC, 1APS, 1AQ5_A, 1ARB, 1AUU_A, 1AUZ, 1AW0, 1AW6, 1AWJ, 1AXH, 1AXJ, 1AYJ, 1AZ6, 1B16_A, 1B1A, 1B22_A, 1B4R_A, 1B64, 1B6F_A, 1B8O_A, 1B8W_A, 1B91_A, 1B9P_A, 1B9U_A, 1BA9, 1BAK, 1BAL, 1BAQ, 1BB8, 1BBG, 1BBI, 1BBN, 1BBY, 1BC6, 1BC9, 1BCI, 1BCT, 1BDC, 1BDS, 1BFM_A, 1BGF, 1BGK, 1BH4, 1BHU, 1BI6_H, 1BIP, 1BJ8, 1BJX, 1BKR_A, 1BKU, 1BL1, 1BLA, 1BLJ, 1BLR, 1BM4_A, 1BMR, 1BMW, 1BMX, 1BNO, 1BNR, 1BO0, 1BO9_A, 1BOE_A, 1BPR, 1BPV, 1BQV, 1BR0_A, 1BRV, 1BRZ, 1BSH_A, 1BT7, 1BUQ_A, 1BUY_A, 1BVE_A, 1BVH, 1BW3, 1BW6_A, 1BW7, 1BXD_A, 1BXO_A, 1BY1_A, 1BYI, 1BYM_A, 1BYQ_A, 1BYY_A, 1BZG, 1BZK_A, 1C01_A, 1C05_A, 1C0P_A, 1C1D_A, 1C1K_A, 1C20_A, 1C2N, 1C3Y_A, 1C4E_A, 1C55_A, 1C5E_A, 1C75_A, 1C7K_A, 1C7U_A, 1C89_A, 1C9Q_A, 1CCH, 1CCM, 1CDB, 1CDQ, 1CE4_A, 1CF4_B, 1CFE, 1CG7_A, 1CHC, 1CHL, 1CK2_A, 1CKV, 1CL4_A, 1CLH, 1CMO_A, 1CMR, 1CN2, 1CO4_A, 1COK_A, 1COO, 1COU_A, 1CUR, 1CW5_A, 1CWW_A, 1CWX_A, 1CX1_A, 1CYE, 1CYU, 1CZ4_A, 1D1D_A, 1D1H_A, 1D6G_A, 1D7Q_A, 1D8B_A, 1D8J_A, 1D8V_A, 1DAQ_A, 1DBD_A, 1DBF_A, 1DCI_A, 1DDF, 1DE1_A, 1DE3_A, 1DEC, 1DEF, 1DFE_A, 1DFS_A, 1DGF_A, 1DGN_A, 1DGQ_A, 1DIP_A, 1DJ0_A, 1DL0_A, 1DL6_A, 1DLX_A, 1DMC, 1DNY_A, 1DP3_A, 1DP7_P, 1DPU_A, 1DQB_A, 1DQC_A, 1DQZ_A, 1DRO, 1DS1_A, 1DS9_A, 1DTV_A, 1DU2_A, 1DU6_A, 1DUJ_A, 1DV0_A, 1DVH, 1DVJ_A, 1DWM_A, 1DX0_A, 1DX7_A, 1DX8_A, 1DXZ_A, 1DZ7_A, 1E01_A, 1E0A_B, 1E0E_A, 1E0H_A, 1E0L_A, 1E0Z_A, 1E17_A, 1E19_A, 1E29_A, 1E2B, 1E3T_A, 1E3Y_A, 1E4U_A, 1E53_A, 1E5G_A, 1E5U_I, 1E68_A, 1E6Q_M, 1E6U_A, 1E7L_A, 1E88_A, 1E8L_A, 1E8R_A, 1ECI_A, 1EDS_A, 1EDV_A, 1EDX_A, 1EF4_A, 1EGX_A, 1EH2, 1EHJ_A, 1EHS, 1EHX_A, 1EIK_A, 1EIT, 1EIW_A, 1EJ5_A, 1EKT_A, 1ELK_A, 1EMW_A, 1ENW_A, 1EO0_A, 1EO1_A, 1EP0_A, 1EQ3_A, 1EQO_A, 1ERC, 1ERD, 1ERX_A, 1ES9_A, 1ESX_A, 1EUW_A, 1EV0_A, 1EWI_A, 1EWS_A, 1EWW_A, 1EXE_A, 1EXG, 1EXK_A, 1EZA, 1EZG_A, 1EZO_A, 1Ezt_A, 1F0Z_A, 1F24_A, 1F3C_A, 1F3R_B, 1F41_A, 1F53_A, 1F5Y_A, 1F81_A, 1F8P_A, 1FA3_A, 1FA4_A, 1FAF_A, 1FBR, 1FCT, 1FCY_A, 1FD8_A, 1FDM, 1FGP, 1FHO_A, 1FJ2_A, 1FJE_B, 1FJK_A, 1FJN_A, 1FM0_D, 1FMH_A, 1FO5_A, 1FP0_A, 1FQQ_A, 1FR3_A, 1FRE, 1FSH_A, 1FU9_A, 1FVL, 1FW9_A, 1FWO_A, 1FWP, 1FWQ_A, 1FYB_A, 1FYC, 1FYJ_A, 1FZT_A, 1G1E_B, 1G25_A, 1G26_A, 1G2H_A, 1G3G_A, 1G4F_A, 1G5V_A, 1G61_A, 1G66_A, 1G6E_A, 1G6S_A, 1G7D_A, 1G7E_A, 1G84_A, 1G90_A, 1G9L_A, 1GAB, 1GD0_A, 1GE9_A, 1GGW_A, 1GH9_A, 1GHC, 1GHH_A, 1GIO, 1GNC, 1GP8_A, 1GW3, 1GYF_A, 1H8C_A, 1HA9_A, 1HBW_A, 1HCD, 1HDO_A, 1HEV, 1HHN_A, 1HKS, 1HNR, 1HP8, 1HPW_A, 1HRE, 1HS7_A, 1HSQ, 1HX2_A, 1HYI_A, 1HYK_A, 1HYW_A, 1HZN_A, 1HZY_A, 1I0H_A, 1I1S_A, 1I25_A, 1I27_A, 1I5G_A, 1I5H_W, 1I5J_A, 1I6W_A, 1IBA, 1IBX_B, 1ICA, 1IHV_A, 1IIE_A, 1IJA_A, 1IL6, 1IMT, 1INZ_A, 1IOJ,

1IRF, 1IRL, 1IRP, 1IRS_A, 1ISU_A, 1ITF, 1IXH, 1JBA_A, 1JHB, 1JLI, 1JOY_A, 1JUN_A, 1JWE_A, 1KDX_A, 1KHM_A, 1KJS, 1KLA_A, 1KOE, 1KRS, 1KSR, 1LEA, 1LRE, 1LXL, 1LYP, 1MFN, 1MGS_A, 1MKC_A, 1MKN_A, 1MLA, 1MNT_A, 1MRO_B, 1MRO_C, 1MUN, 1MUT, 1MYF, 1NCS, 1NCT, 1NEQ, 1NGL_A, 1NGR, 1NKL, 1NLS, 1NOE, 1NS1_A, 1NTC_A, 1OAA, 1OLG_A, 1OM2_A, 1PA2_A, 1PAA, 1PCE, 1PCN, 1PCP, 1PEH, 1PFL, 1PFS_A, 1PIH, 1PIR, 1PLS, 1PMC, 1PMS, 1PNB_A, 1PNB_B, 1PNJ, 1PON_B, 1POU, 1PRR, 1PSM, 1QA5_A, 1QCE_A, 1QCK_A, 1QDP, 1QFD_A, 1QFQ_B, 1QFR_A, 1QFT_A, 1QGP_A, 1QH4_A, 1QHK_A, 1QJO_A, 1QK6_A, 1QK7_A, 1QK9_A, 1QKF_A, 1QKL_A, 1QKS_A, 1QL0_A, 1QLO_A, 1QM9_A, 1QN0_A, 1QND_A, 1QNR_A, 1QOP_B, 1QP6_A, 1QQF_A, 1QQI_A, 1QQV_A, 1QRJ_B, 1QRY_A, 1QSV_A, 1QTN_A, 1QTN_B, 1QTO_A, 1QTS_A, 1QTT_A, 1QTW_A, 1QU5_A, 1QU6_A, 1QYP, 1R2A_A, 1RAX_A, 1RCH, 1RCS_A, 1RES, 1RGE_A, 1RIE, 1RIP, 1ROT, 1RPR_A, 1RRB, 1RXR, 1SAP, 1SCY, 1SGG, 1SHC_A, 1SRO, 1SSN, 1SUH, 1SVF_A, 1SVF_B, 1SVQ, 1SWU_A, 1TBA_A, 1TBA_B, 1TBD, 1TBN, 1TFB, 1THF_D, 1TLE, 1TNS, 1TOF, 1TPM, 1TRL_A, 1TSG, 1U2F_A, 1UMS_A, 1URK, 1UTR_A, 1UWO_A, 1UXC, 1VGH, 1VPU, 1VRE_A, 1WDB, 1WFB_A, 1WHI, 1XBL, 1XNA_A, 1XNB, 1XPA, 1YGE, 1YUA, 1YUB, 1YUI_A, 1ZTA, 1ZTO, 2A3D_A, 2ALC_A, 2BID_A, 2CTC, 2END, 2EZH, 2EZK, 2EZM, 2FMR, 2GAT_A, 2GCC, 2GVA_A, 2HGF, 2HIR, 2HMX, 2IF1, 2IFE_A, 2IFO, 2JHB_A, 2LFB, 2LIS_A, 2MRB, 2NCM, 2NLR_A, 2OLB_A, 2ORC, 2PCF_B, 2PRF, 2PTH, 2PTL, 2REL, 2SOB, 2TMP, 2TPS_A, 2U2F_A, 2VIK, 3CHB_D, 3CRD, 3LRI_A, 3MEF_A, 3MSP_A, 3PHY, 3RPB_A, 3SIL, 3VUB, 3ZNF, 4EUG_A, 4ULL, 5GCN_A, 7A3H_A.

¹M. E. Davis and J. A. McCammon, *Chem. Rev.* **90**, 509 (1990); R. M. Levy and E. Gallicchio, *Annu. Rev. Phys. Chem.* **49**, 531 (1998).

²B. Honig and A. Nicholls, *Science* **268**, 1144 (1995).

³J.-H. Lin, N. A. Baker, and J. A. McCammon, *Biophys. J.* **83**, 1374 (2002); G. S. D. Ayton, S. Bardenhagen, P. McMurry, D. Sulsky, and G. A. Voth, *IBM J. Res. Dev.* **45**, 417 (2001).

⁴B. Roux, *Biophys. J.* **73**, 2980 (1997).

⁵W. Im, M. Feig, and C. L. Brooks III, *Biophys. J.* **85**, 2900 (2003).

⁶D. S. Goodsell, *Trends Biochem. Sci.* **16**, 203 (1991).

⁷E. Liepinsh, G. Otting, and K. Wuethrich, *Nuc Acids Res* **20**, 6549 (1992); H. R. Drew and R. E. Dickerson, *J. Mol. Biol.* **151**, 535 (1981); M. Feig and B. M. Pettitt, *ibid.* **286**, 1075 (1999).

⁸D. Sitkoff, K. A. Sharp, and B. Honig, *J. Phys. Chem.* **98**, 1978 (1994).

⁹E. Gallicchio, L. Y. Zhang, and R. M. Levy, *J. Comput. Chem.* **23**, 517 (2002).

¹⁰C. J. Cramer and D. G. Truhlar, *Chem. Rev.* **99**, 2161 (1999); B. Roux and T. Simonson, *Biophys. Chem.* **78**, 1 (1999); M. K. Gilson, *Curr. Opin. Struct. Biol.* **5**, 216 (1995).

¹¹J. D. Jackson, *Classical Electrodynamics* (Wiley, New York, 1999).

¹²R. Constanciel and R. Contreras, *Theor. Chim. Acta* **65**, 1 (1984).

¹³W. C. Still, A. Tempczyk, R. C. Hawley, and T. Hendrickson, *J. Am. Chem. Soc.* **112**, 6127 (1990).

¹⁴M. Feig, A. Onufriev, M. S. Lee, W. Im, D. A. Case, and C. L. Brooks III, *J. Comput. Chem.* (in press).

¹⁵M. S. Lee, F. R. Salsbury, Jr., and C. L. Brooks III, *J. Chem. Phys.* **116**, 10606 (2002).

¹⁶M. S. Lee, M. Feig, F. R. Salsbury, Jr., and C. L. Brooks III, *J. Comput. Chem.* **24**, 1348 (2003).

¹⁷A. Ghosh, C. S. Rapp, and R. A. Friesner, *J. Phys. Chem. B* **102**, 10983 (1998); W. Im, M. S. Lee, and C. L. Brooks III, *J. Comput. Chem.* **24**, 1691 (2003).

¹⁸A. Onufriev, D. Bashford, and D. A. Case, *J. Phys. Chem. B* **104**, 3712 (2000).

¹⁹B. N. Dominy, D. Perl, F. X. Schmid, and C. L. Brooks III, *J. Mol. Biol.* **319**, 541 (2002); B. N. Dominy and C. L. Brooks III, *J. Phys. Chem. B* **103**, 3765 (1999); A. Onufriev, D. A. Case, and D. Bashford, *J. Mol. Biol.* **325**, 555 (2003); M. Feig, A. D. MacKerell, Jr., and C. L. Brooks III, *J. Phys. Chem. B* **107**, 2831 (2003); N. Calimet, M. Schaefer, and T. Simonson, *Proteins* **2001**, 144; L. Y. Zhang, E. Gallicchio, R. A. Friesner, and R. M. Levy, *J. Comput. Chem.* **22**, 591 (2001); V. Tsui and D. A. Case, *J. Am. Chem. Soc.* **122**, 2489 (2000).

²⁰J. Zhu, Y. Shi, and H. Liu, *J. Phys. Chem. B* **106**, 4844 (2002).

²¹B. N. Dominy and C. L. Brooks III, *J. Comput. Chem.* **23**, 147 (2001); M. Feig and C. L. Brooks III, *Proteins* **49**, 232 (2002); A. K. Felts, E. Gallicchio, A. Wallqvist, and R. M. Levy, *ibid.* **48**, 404 (2002).

²²B. Jayaram, Y. Liu, and D. L. Beveridge, *J. Chem. Phys.* **109**, 1465 (1998).

²³K. L. Mardis, R. Luo and M. K. Gilson, *J. Mol. Biol.* **309**, 507 (2001).

²⁴V. Z. Spassov, L. Yan, and S. Szalma, *J. Phys. Chem. B* **106**, 8726 (2002).

²⁵M. Born, *Z. Phys.* **1**, 45 (1920).

²⁶M. Schaefer and M. Karplus, *J. Phys. Chem.* **100**, 1578 (1996).

²⁷D. Bashford and D. A. Case, *Annu. Rev. Phys. Chem.* **51**, 129 (2000).

²⁸J. G. Kirkwood, *J. Chem. Phys.* **2**, 351 (1934).

²⁹P. H. Hönenberger and W. F. van Gunsteren, *J. Chem. Phys.* **108**, 6117 (1998).

³⁰W. Im, D. Beglov, and B. Roux, *Comput. Phys. Commun.* **111**, 59 (1998).

³¹M. Nina, D. Beglov, and B. Roux, *J. Phys. Chem.* **101**, 5239 (1997).

³²B. R. Brooks, R. E. Bruccoleri, B. D. Olafson, D. J. States, S. Swaminathan, and M. Karplus, *J. Comput. Chem.* **4**, 187 (1983).

³³A. Nicholls and B. Honig, *J. Comput. Chem.* **12**, 435 (1991).

³⁴A. D. MacKerell, Jr., D. Bashford, M. Bellott *et al.*, *J. Phys. Chem. B* **102**, 3586 (1998).

³⁵M. Feig, J. Karanicolas, and C. L. Brooks III, *J. Mol. Graphics Modell* (in press).

³⁶H. M. Berman, J. Westbrook, Z. Feng, G. Gilliland, T. N. Bhat, H. Weissig, I. N. Shindyal, and P. E. Bourne, *Nucl. Acids Res.* **28**, 235 (2000).

³⁷A. Kolinski and J. Skolnick, *Proteins* **32**, 475 (1998).

³⁸M. Feig, P. Rotkiewicz, A. Kolinski, J. Skolnick, and C. L. Brooks III, *Proteins* **41**, 86 (2000).

³⁹A. Onufriev, D. A. Case, and D. Bashford, *J. Comput. Chem.* **23**, 1297 (2002).